applied sciences

Article

Determination of Hazardous Zone of Coal Spontaneous Combustion in Ultra-Long Working Face Based on the Gob Porosity Evolution and Flow Field Distribution

Shuliang Xie [1], Gang Wang [1,2,*], Enmao Wang [1], Qiming Huang [1] and Mingze Xia [1]

1 College of Safety and Environmental Engineering, Shandong University of Science and Technology, Qingdao 266590, China
2 Mine Disaster Prevention and Control-Ministry of State Key Laboratory Breeding Base, Shandong University of Science and Technology, Qingdao 266590, China
* Correspondence: gang.wang@sdust.edu.cn

Abstract: Coal fire remains one of the main hazards of underground work. Spontaneous coal fires cause serious casualties and property losses. At present, most of the studies on coal spontaneous combustion have been conducted on working faces shorter than 200 m. However, the ultra-long working face gob of shallow buried coal seam is much larger, the distribution of its flow field is more complex, and, thus, risk of spontaneous combustion in the gob is higher. Exploring the evolution law of the gob flow field of ultra-long working face to quickly determine the range of the coal spontaneous combustion hazardous zone is of great significance to the safe production of similar mines. In this study, the gas flow field distribution in the gob of an ultra-long working face was measured by buried pipeline method and oxygen concentration was used as the index. It is found that the oxygen concentration decreases with the advance of the working face. Based on the flow field distribution, the oxidation zone of the gob was determined. Meanwhile, a three-dimensional (3D) numerical model of the working face was established, and the overlying stratum collapse and porosity evolution in the gob were simulated using the particle flow software, PFC^{3D} discrete element software, for the porosity distribution law of the gob. The obtained porosity data were then imported into FLUENT using the custom function UDF to construct a 3D grid model. The flow field distribution in the gob was then numerically simulated for the seepage and migration law of the wind flow in the gob. The results reveal an arch-shaped wind flow field distribution with a swirl shape on the intake airway side. In the strike direction, the wind flow gradually becomes weaker with the advance of the working face. In the dip direction, the wind flow seepage range on the return airway side is obviously higher than that on the intake airway side. In the vertical direction, the wind flow range in the upper gob is larger than that in the middle and lower gob. The spontaneous combustion and oxidation zone of the gob is determined to be at 140.4–313.3 m on the intake airway side, 201.2–351.6 m in the middle of the gob, and 153.2–328.1 m on the return airway side. Finally, the residual coal distribution was superimposed onto the oxygen concentration distribution to obtain the spontaneous residual coal combustion hazardous zone in the gob.

Keywords: coal; autoignition; ultra-long working face; porosity; PFC-CFD; hazardous zone

check for updates

Citation: Xie, S.; Wang, G.; Wang, E.; Huang, Q.; Xia, M. Determination of Hazardous Zone of Coal Spontaneous Combustion in Ultra-Long Working Face Based on the Gob Porosity Evolution and Flow Field Distribution. *Appl. Sci.* **2023**, *13*, 4574. https://doi.org/10.3390/app13074574

Academic Editors: Changliang Han and Xiaoqing Wang

Received: 17 March 2023
Revised: 30 March 2023
Accepted: 31 March 2023
Published: 4 April 2023

1. Introduction

With the developments of economy, science, and technology, the world energy structure has changed and clean energies, such as solar energy and wind energy, are included in the new energy development strategy. Yet coal is still the most abundant and widely used energy source on the Earth [1–3]. In recent years, the safety of coal mine production has been improved and gradually stabilized, yet there are still a large number of coal mine accidents, among which coal fire accidents are most frequent [4,5].

For a long time, coal fire has been one of the main hazards in underground coal mining workplaces, and the spontaneous combustion of residual coal in gob is the main contributor to coal fire [6,7]. The main internal factor of coal spontaneous combustion is the spontaneous combustion propensity of coal, while the factor determining the spontaneous combustion propensity of coal is the coal petrographic composition [8–10]. Domestic and foreign scholars have proposed several methods to identify the spontaneous combustion propensity of coal based on different identification techniques. Antoshenko [11,12] has tested and obtained the industrial analysis parameters of coal through corresponding identification techniques, and divided the spontaneous combustion propensity grade of coal. Coal fire is the most unpredictable hazard and most difficult to be controlled because it often occurs in the gob [13]. Therefore, how to quickly locate the coal spontaneous combustion in gob and accurately implement targeted measures is of great significance to ensure safe production in mines.

To clearly identify the hazardous areas of spontaneous residual coal combustion, a field test method has been established by monitoring the gas distribution in the gob and the concept of "three zones", namely the heat dissipation zone, the oxidation zone, and the suffocation zone, is proposed. The division of the oxidation zone and suffocation zone using oxygen concentration can usually result in an accurate boundary. Xie et al. [14] measured the oxygen concentration using buried tubes and determined the range of the gob spontaneous combustion "three zones" based on the oxygen concentration distribution and temperature rise. Wen et al. [15] identified the range of spontaneous combustion "three zones" in the gob of a super long fully mechanized mining fac during the withdrawal based on oxygen concentration and the thickness of the floating coal.

Due to certain limitations in on-site observation, CFD software has been widely used to characterize the flow field in coal seam gob. Worf [16] studied the oxygen distribution in coal seam gob by combining CFD and field measurements and determined the spontaneous combustion hazardous areas. Magdalena [17] thoroughly analyzed the gas seepage characteristics in the goaf of a fully mechanized mining face with a U-shaped ventilation system through CFD software, determined the critical values of the seepage velocity and oxygen concentration in the goaf, established a mathematical model for coal spontaneous combustion, and simulated and calculated the gas concentration index in the upper corner of the distribution of the spontaneous combustion hazard area in the goaf, establishing a composite risk assessment model. Zhuo [18] aimed at the impact of porosity and overlying rock fractures in the goaf on the coal spontaneous combustion risk zone, taking Bulianta Coal Mine as the background, introduced the model into the FLUENT software, and conducted numerical simulation of the O_2 concentration field, CO concentration field, and wind speed field in the goaf. The simulation results are in good agreement with the on-site measured data. Cheng [19] et al. quantitatively simulated gob porosity distribution from the microscopic point of view by the discrete element method (DEM) and wrote a user-defined function (UDF) code that was then substituted into CFD to simulate the gas distribution in gob. The results indicated that that gas was mainly distributed in the upper gob. Gao et al. [20] simulated the gob flow field distributions under different porosity conditions and confirmed that porosity change directly affected gob flow field. The change characteristics of gob porosity are also affected by the complex distribution and collapse of the overlying strata. Under these influences, it is difficult to obtain the accurate porosity. Numerous studies reveal that numerical simulation is a good tool for studying rock formation failure mechanism and porosity change. Hu et al. [21] comprehensively studied the fracture development law of overlying rock in the working face during caving by similarity simulation, theoretical analysis, and field measurement. Di et al. [22] explored the failure characteristics and stress evolution law of overburden strata during caving using the COMSOL numerical simulation software. By the physical experiments on similar materials and particle flow numerical simulation, Wang et al. [23] established a mathematical model of the tensile deformation of rock formation and the gas-conducting fracture zone. They innovatively measured the porosity using the discrete element Particle Flow Code (PFC) software to accurately divide the gas-enriched area and revealed the evolution law of fracturing expansion–penetration of fracture in the overlying strata of gob. In addition to the PFC and CFD methods, Gamy [24] and others used pneumatic control automation systems to identify coal spontaneous combustion heat sources in coal mining faces.

Most of the studies on the spontaneous combustion hazardous area in coal seam gob focus on the working faces shorter than 200 m and there are very few studies on the flow fields in the gobs behind ultra-long working faces. With the mechanization of caving, most working faces have been extended to more than 200 m. Due to the strike and long working face in the strike direction, there is a large amount of residual coal left in the large gob, which provides the material conditions for coal spontaneous combustion. In addition, most working faces adopt gob-side entry retaining (GER) technology, which results in large air leakage in the gob and complicated air leakage channels to provide a good oxygen supply environment for the oxidation of residual coal, resulting in a higher risk of spontaneous combustion. Therefore, studying the gob flow field behind an ultra-long working face and clearly defining the hazardous zone of spontaneous combustion in the gob have strong guiding significance for coal fire prevention and extinguishing in similar mines.

2. Research Methods and Means

This study took the 31,116 fully mechanized working face with GER of Jinjie Coal Mine as the research object. The parameters of the working face are shown in Table 1.

Table 1. Working face parameters (own elaboration).

Name	Dip Length	Strike Length	Average Thickness	Mining Method	Lithology of Coal Seam Roof and Floor
31,116 fully mechanized caving face	335.9 m	5126 m	3.33 m	full-seam mining	sandstone and mudstone

The gob gas distribution was determined by field measurement. The gob flow field was characterized using the PFC software and the CFD finite element software. Based on the simulation results obtained with the two software, the spontaneous combustion hazardous zone in the gob was determined to provide a theoretical basis for coal spontaneous combustion prevention.

2.1. Field Measurement of Gob Gas Distribution

The gas in the gob of 31,116 working face was sampled using the buried bundle tube and high-pressure rubber hose at 4 points to determine the gas distribution. The roadway layout of the working face is shown in Figure 1a. The working face adopts the technology of gob-side entry retaining and the working face is adjacent to the goaf of working face 31,115 and the preparation working face 31,117. Figure 1b shows the arrangement of the 4 measuring points, with one on the intake airway side (1#), one on the return airway side (4#), and two in the middle of the working face (2# and 3#). The sampling on the 4# measuring point was conducted with the bundle tube on top of the return airway and the gas samples at other three points were collected with more flexible high-pressure hoses. To lay the monitoring pipelines between the working face supports, high-pressure rubber hoses were wound on the supports hung on the hydraulic support and fixed using clamps to prevent falling and ensure smooth rotation during the support movements. The high-pressure hose was released and buried in the gob as the working face advanced.

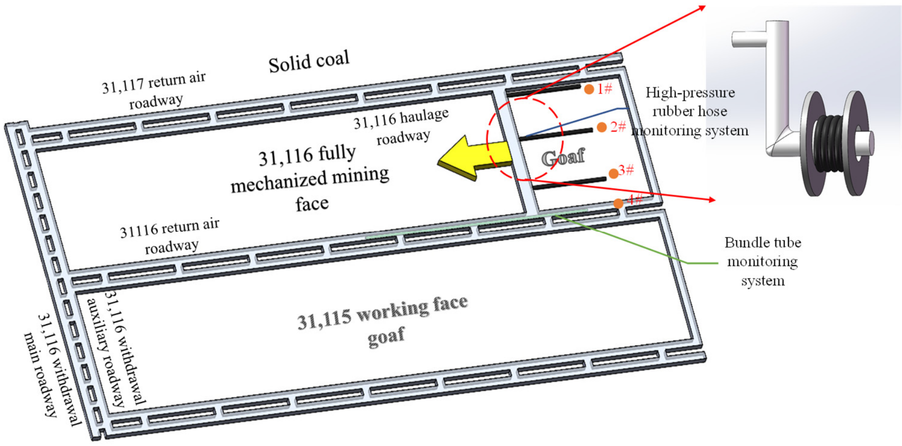

(**a**)

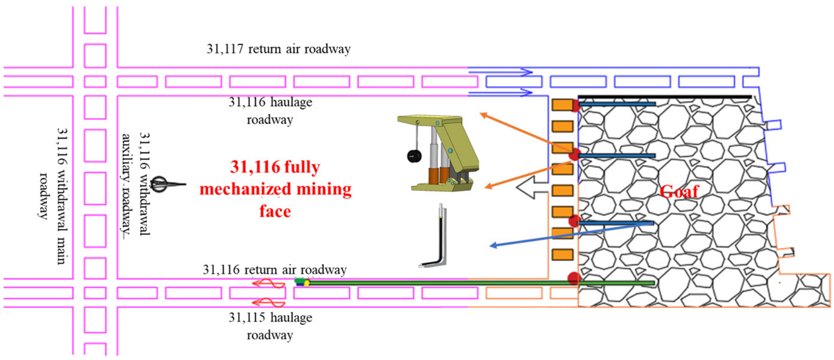

(**b**)

Figure 1. Monitoring pipeline layout in the three zones of gob (own elaboration). (**a**) Roadway layout of 31,116 fully mechanized working face. (**b**) Plan view of the three zones of gob with monitoring pipelines buried.

2.2. PFC-FLUENT Numerical Simulation of Gob Flow Field

2.2.1. Macroscopic and Mesoscopic Parameters and DEM Model Construction

Calculation of macro- and micro-parameters

Selecting and calculating appropriate macroscopic and mesoscopic parameters are important steps in the model construction for PFC simulation [25]. Bonded particle models are divided into contact bond models and parallel bond models. A parallel bond model can more realistically simulate coal-like materials in tension or shear fracture and, thus, is selected for simulation in this work. Referring to the mesoscopic parameters of rock materials based on the principle of particle flow measurement, the following empirical formulas were used to calculate the parameters for PFC numerical simulation.

(1) Empirical formula of elastic modulus:

$$E/E_c = a + b\ ln(k_n/k_s) \quad (1)$$

where E is the elastic modulus, GPa; E_c is the Young's modulus, GPa; k_n/k_s is the stiffness ratio; a = 1.652; and b = −0.395.

(2) Poisson's ratio empirical formula:

$$v = c\, ln(k_n/k_s) + d \tag{2}$$

where v is Poisson's ratio; c = 0.209; and d = 0.111.

(3) Regression analysis of uniaxial compressive strength:

$$\frac{\sigma_c}{\overline{\sigma}} = \begin{cases} a\left(\frac{\overline{\tau}}{\overline{\sigma}}\right)^2 + b\frac{\overline{\tau}}{\overline{\sigma}},\ 0 < \frac{\overline{\tau}}{\overline{\sigma}} \le 1 \\ c \quad ,\ \frac{\overline{\tau}}{\overline{\sigma}} > 1 \end{cases} \tag{3}$$

where σ_c is the compressive strength, MPa; $\overline{\sigma}$ is the normal connection strength of parallel connection, MPa; τ is the tangential connection strength of parallel connection, MPa; a = −0.965; b = 2.292; and c = 1.327.

(4) Regression analysis of tensile strength:

$$\frac{\sigma_t}{\overline{\sigma}} = \begin{cases} d\left(\frac{\overline{\tau}}{\overline{\sigma}}\right)^2 + e\frac{\overline{\tau}}{\overline{\sigma}},\ 0 < \frac{\overline{\tau}}{\overline{\sigma}} \le 1 \\ f \quad ,\ \frac{\overline{\tau}}{\overline{\sigma}} > 1 \end{cases} \tag{4}$$

where σ_t is tensile strength, MPa; d = −0.174; e = 0.463; and f = 0.289.

The calculated macroscopic and mesoscopic parameters are shown in Table 2.

Table 2. Macroscopic and mesoscopic physical and mechanical properties of rock formations (access to information).

Formations	Rock	Macro Parameters					Micro Parameters					
		μ	E	Rm/MPa	Cohesion /MPa	Angle of Internal Friction /(°)	Krat	Emod /GPa	Kn /GPa	Ks /GPa	Pb-Kn /GPa	Pb-Ks /GPa
J6	Medium Grained Sandstone	0.17	11.75	2.58	4.35	35.3	1.4	20.1	40.2	28.5	24.6	18.1
J5	Siltstone	0.15	19.5	1.84	2.75	36	1.8	12.7	25.4	14.3	15.8	9
J4	Mudstone	0.26	8.57	0.605	1.2	39.4	1.2	4.5	9	7.4	5.6	4.7
J3	Coal	0.3	5.3	0.15	1.25	42.6	2.1	5.1	9.2	4.7	6.3	2.9
J2	Sandy mudstone	0.147	10.85	3.6	2.5	35.4	1.2	4.6	9.2	7.6	5.7	4.7
J1	Siltstone	0.15	19.5	2.01	2.45	36	1.8	12.7	25.4	14.3	15.8	9

PFC model and boundary conditions

The mining process of 31,116 working face in Jinjie Coal Mine was simulated and analyzed using the PCF^{3D} software. Based on the geological histogram of the coal seam, a numerical model was established by the radius expansion method, as shown in Figure 2a. The original size of the working face leads to a very large model and a large number of particles, which makes the calculation difficult, calculation time long, and results inaccurate. Therefore, the model size was reduced in proportion to 106 m long, 67.18 m wide, and 20.51 m high, with a total of 6 floors. Because the average dip angle of the coal seam is 1°, the upper boundary of the model is a free boundary, and the left and right boundaries are fixed. The particles are allowed to move in the vertical direction, and the bottom boundary restricts their movement in the vertical direction. The particle sizes of the model are in the range of 0.6–0.8, with reasonable size ratio. The mining process is shown in Figure 2b and is divided into 10 mining steps. Each mining step records the overlying rock collapse and porosity changes.

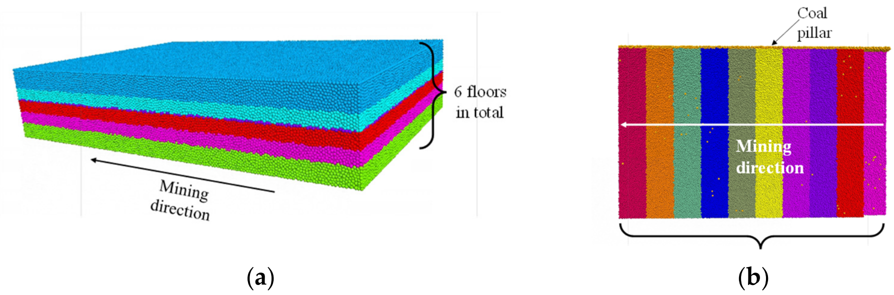

Figure 2. PFC model and caving process of the coal seam model (own elaboration). (**a**) Three-dimensional (3D) numerical model diagram. (**b**) Schematic diagram of caving process.

2.2.2. CFD Model and Boundary Conditions

The gob flow field and gas distribution of the working face were simulated using the ANSYS Fluent software. Fluent is a CFD calculation software used to simulate the fluid flows and heat conductions in complex shapes. It is highly efficient and accurate.

A simplified 3D grid model of fully mechanized mining gob was established using the basic parameters of the 31,116 working face in Jinjie Coal Mine. First, based on the real size of the working face, a 3D model was constructed using the Solidworks software, with the length, width, and height of the gob set to 500 m, 336 m, and 50 m, respectively. To meet the requirement of the later simulation, structural hexahedral meshing was conducted using the ICEM-CFD software to construct the 3D grid model as shown in Figure 3.

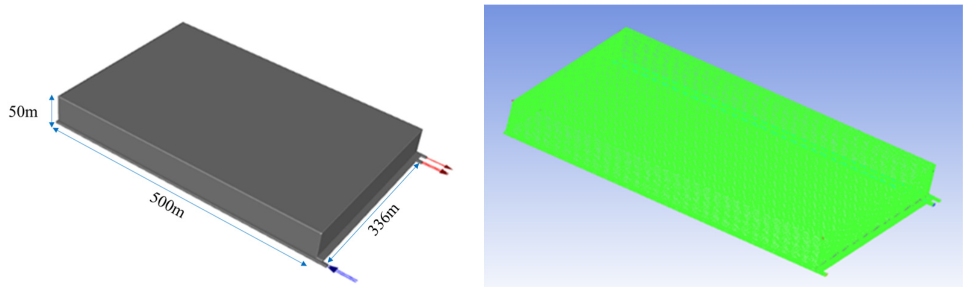

Figure 3. The 3D model and grids of gob in working face (own elaboration).

The mesh quality will directly affect the accuracy and convergence speed of the Fluent numerical simulation. As shown in Figure 4 for the mesh quality examination histogram, the mesh qualities range from 0.981 to 1, meeting the requirements of FLUENT calculation.

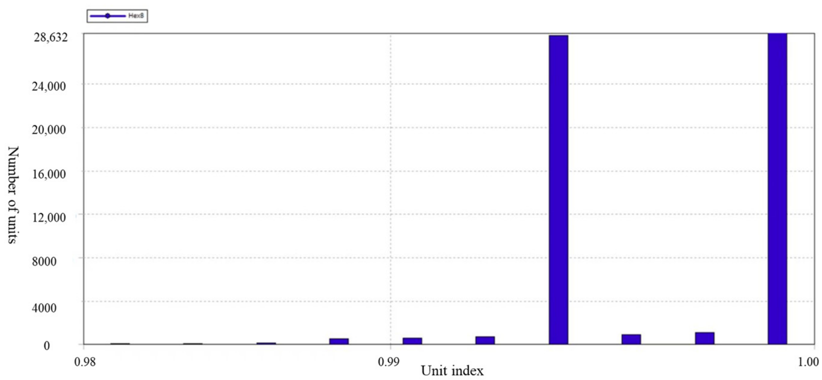

Figure 4. Mesh quality distribution diagram (own elaboration).

The inlet of the intake airway of the working face is defined as the velocity inlet, and the boundary condition type is velocity inlet. The outlet of the return airway is defined as the outflow. The two surfaces between the working face and the gob are defined as the interior. The entire 3D model is defined as fluid in ICEM-CFD. The calculation conditions are then initialized to conduct the iterative calculation for numerical simulation.

3. Results

3.1. Field Measurement Results of Gas Distribution

After the gas monitoring pipelines were installed in the gob, a gas sample was collected at each measuring point every day at the same time during the normal working face caving and analyzed by gas chromatograph for oxygen concentration.

The definition of an oxidation zone is generally based on three parameters, air leakage speed, temperature rise rate, and oxygen concentration in the gob. The first two are mostly used in theoretical calculations and are significantly affected by caving conditions. In particular, it is difficult to obtain the actual temperature rise rate and air leakage speed of a gob. Therefore, in this study, an area with the oxygen concentration in the range of 8–18% is defined as an oxidation zone. The measured oxygen concentrations on the intake airway side, the middle, and the return airway side of the gob were classified, compared, and analyzed.

As can be seen from Figure 5, the oxygen concentration in the goaf generally presents a downward trend but there is a certain fluctuation phenomenon. This is mainly due to the complex law of air leakage along the gob-side entry retaining. In addition, due to the different temperatures each day, the underground air pressure is different and the changes in natural wind pressure will also lead to the distribution of oxygen in the goaf. Figure 5a shows that, when the 1# measuring point advanced to 136.4 m, the oxygen concentration drops from 18.76% to 17.07% and the point evolves from heat dissipation zone to oxidation zone. When the 2# measuring point advanced to 158.1 m, the oxygen concentration drops from 20% to 17.94% and it enters the oxidation zone from the heat dissipation zone. According to Figure 5b, because its position is close to the return airway, the 3# measuring point does not enter the oxidation zone from the heat dissipation zone until advancing to 210.2 m. At this point, the oxygen concentration drops from 18.62% to 17.72%. The oxygen concentration at 4# measuring point in the return airway also shows a decreasing trend as the working face advanced. It enters the oxidation zone as it advances to 160.1 m when the oxygen concentration drops from 19.29% to 17.85%. It can be explained that the oxidation of residual coal in the gob gradually consumes the oxygen, and the fresh air flow cannot effectively compensate for the consumed oxygen through the air leakage channel. In addition, the oxidation gradually reduces the amount of residual coal available for the reaction. Therefore, due to the limitation of field conditions, it is difficult to accurately define the range of gob spontaneous combustion "three zones" only by field measurement. It is necessary to conduct numerical simulation to explore the gob flow field distribution law of the ultra-long working face. The field measurement results can function as the foundation for the subsequent study on the gob porosity and flow field.

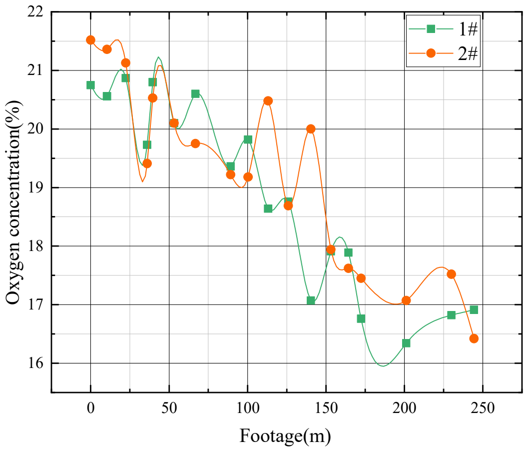

(a)

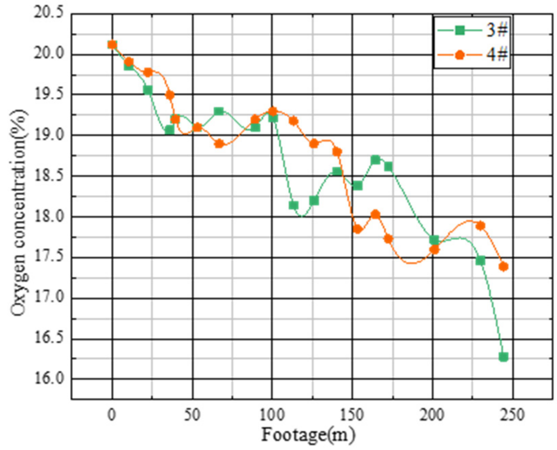

(b)

Figure 5. Oxygen concentration distribution at each measuring point (own elaboration).

3.2. Overlying Stratum Collapse Law and Porosity Simulation

The coal seam was divided into 10 blocks in the caving direction and the blocks were sequentially extracted in the caving direction to simulate the overlying stratum collapse and porosity evolution during caving. As shown in Figure 6a, the first block caving already makes the immediate roof loose, resulting in fractures, yet it still can provide support to the overlying stratum. The primary roof and the height of each floor remain unchanged. As shown in Figure 6b, the caving of the second block enhances the stress on the primary roof. The roof cannot provide the supporting function and collapses. The number of cracks in the overlying stratum continuously increases. As shown in Figure 6c, after the caving of the third block, the immediate roof of the first block has collapsed and that on the second block is loosened yet not collapsed. As shown in Figure 6d–i, starting from the third block, the roofs and overlying strata in the previous gob blocks collapse after each block caving, but the immediate roof of the previous block of the current block is loosened but does not collapse. As shown in Figure 6j, the simulation is finished at the caving of the 10th block. The growth rate of fracture in each stratum slows down but the number of fractures continues to increase. Once the collapse in the gob is finished, the fallen rock piles up and the number of fractures decrease to a stable value.

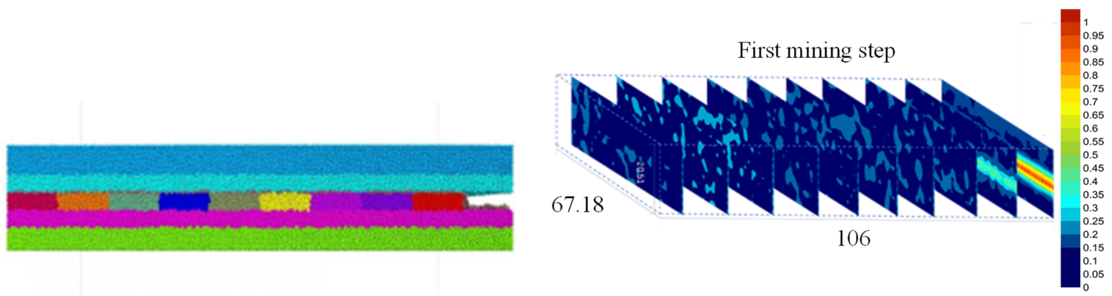

(a)

Figure 6. *Cont.*

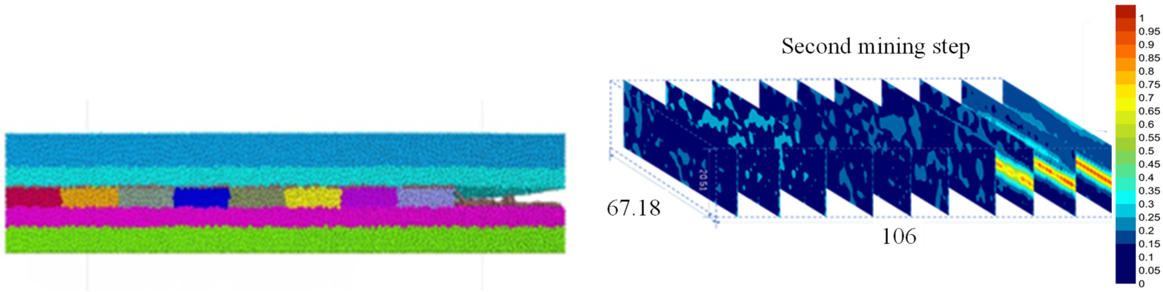

(**b**)

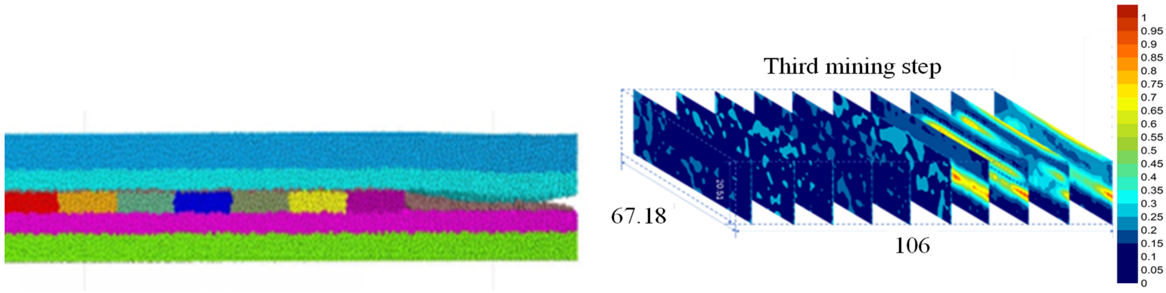

(**c**)

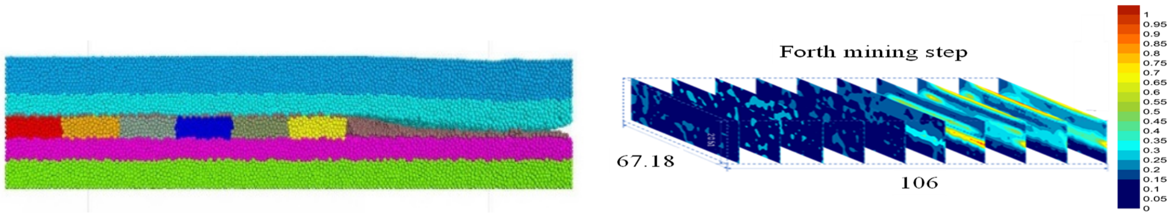

(**d**)

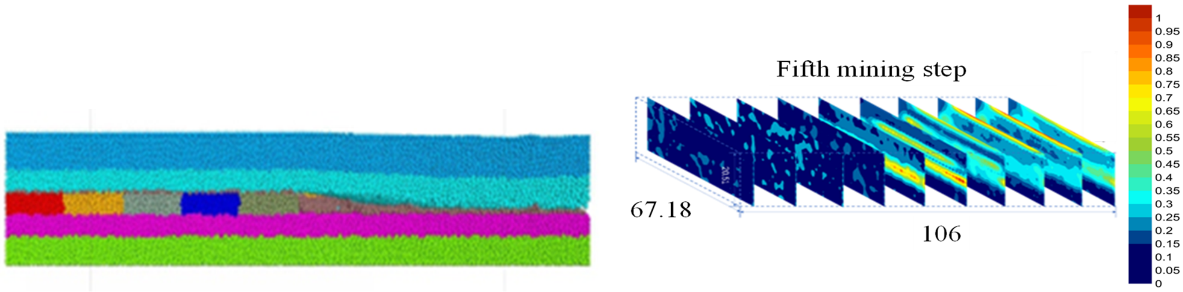

(**e**)

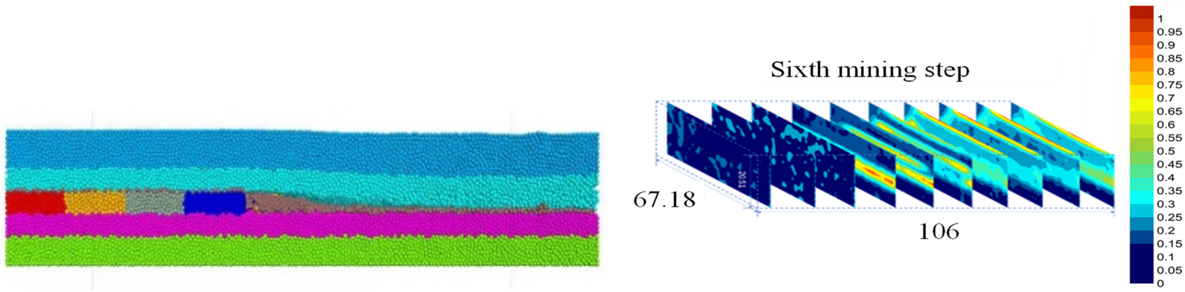

(**f**)

Figure 6. *Cont.*

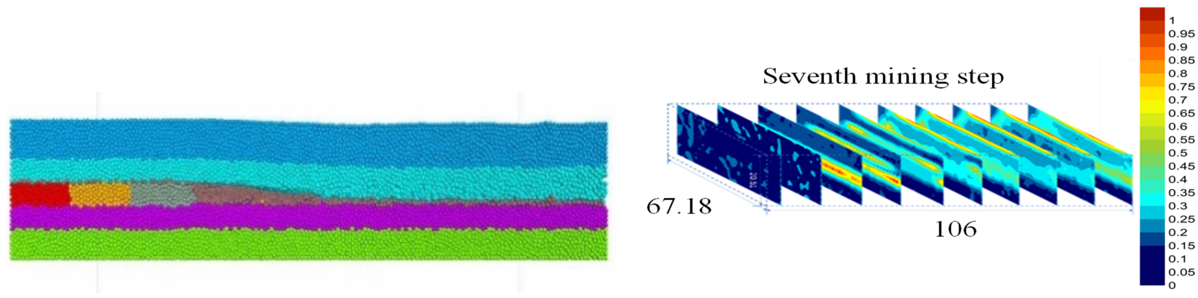

(**g**)

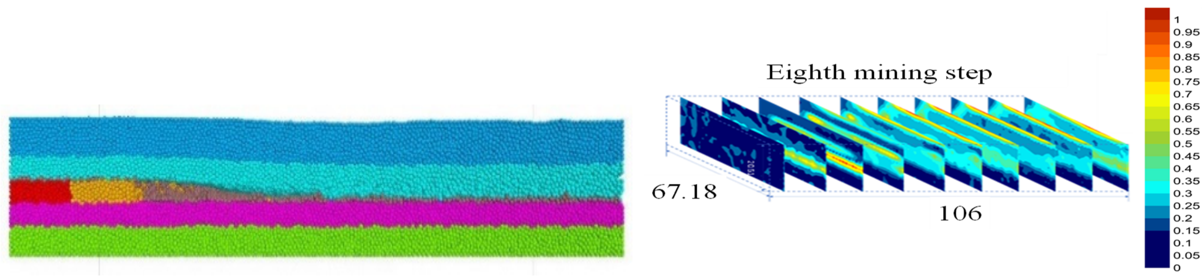

(**h**)

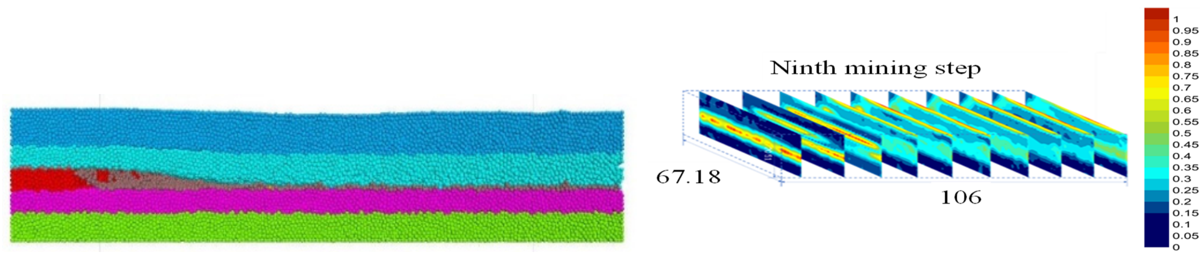

(**i**)

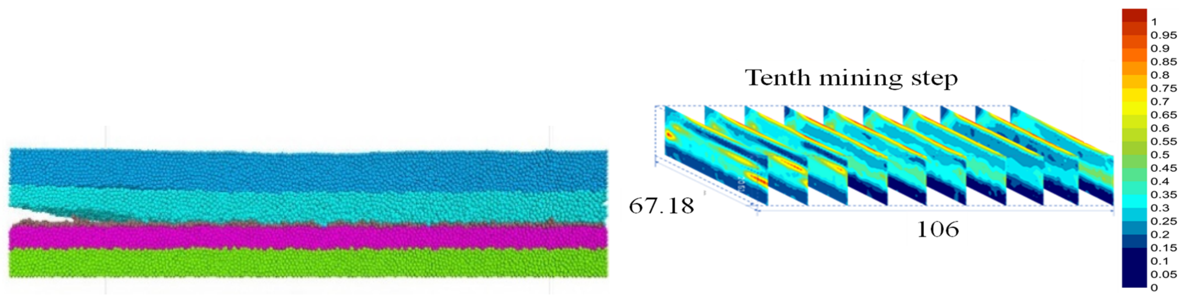

(**j**)

Figure 6. Overlying stratum collapse and porosity change pattern during coal seam caving (own elaboration). (**a**) First caving step. (**b**) Second caving step. (**c**) Third caving step. (**d**) Fourth caving step. (**e**) Fifth caving step. (**f**) Sixth caving step. (**g**) Seventh caving step. (**h**) Eighth caving step. (**i**) Ninth caving step. (**j**) Tenth caving step.

Based on the simulation results of overlying stratum collapse situation, the gob of the 31,116 working face can be regarded as porous medium space. The relevant parameters of this porous medium are then determined and the corresponding equations are established for simulation, calculation, and analysis. The simulation of caving face dynamically tracks the changes in the model porosity during the caving process using measurement circles and the data at each time node are processed for dynamic porosity change of the entire model to summarize the gob porosity evolution law.

The overlying stratum collapse and gob porosity in each caving step is analyzed as shown in Figure 6. The porosities of the unmined coal seam and overlying stratum are small, ranging from 0.15 to 0.3, and their distribution is relatively uniform. As the working face is caved, the overlying stratum keeps collapsing and accumulates with the advancement of the working face, which changes the gob porosity. The porosity changes during the 10 caving steps in Figure 6 suggest that the coal seam is in an unexploited state at the first caving step. The porosity shows the blue original state with the value of 0.1, and there are no obvious changes observed in the overlying stratum and key floors. By the fourth caving step, e.g., almost halfway through, the porosity is greatly changed. In the coal seam, the working face is in the stress-reduced zone and the immediate roof dose not collapse, resulting in the red–yellow area with porosity of about 0.75–0.95. The uncollapsed ranges at two ends of the working face are longer than other positions due to the supporting effect of the coal pillars on the roof and, thus, the red and yellow areas at the two ends are more obvious. The roof collapses at other positions in the gob are basically stable, resulting in porosities ranging from 0.25 to 0.55. The upper immediate roof near the working face shows no collapses but obvious cracks are formed, resulting in the porosity increasing from the original 0.12 to 0.21. The immediate roof above the gob behind the working face completely collapses and the porosity of the area is stable at 0.45, 3.5 times that of the unmined area. The area shows yellow–green color in the figure.

The simulation results of overlying stratum collapse and porosity evolution suggest that, after the third caving step is completed, that is, when the working face advances to ~160 m, the first gob block enters the load-affected zone of the horizontal "three-zone". Although the overlying stratum has collapsed, the porosity here is still relatively large. This is because the gravity of the overlying stratum cannot fully act on the residual coals and gangue in the gob due to the supporting effect of the hinged rock beams, and thus cannot well compact the residual coals and gangue, leaving a certain number of pores. A certain amount of air flow can leak into the gob through these pores. Yet the wind flow speed is relatively low, which cannot bring the heat generated by the oxidation of residual coal away, resulting in more heat generation than heat loss. If the advancement of the working face is slow and the heat accumulation is long enough, the spontaneous combustion of residual coal will occur. The porosity of this area decreases significantly after the working face advances to the fourth block because it enters the compaction zone of the horizontal "three-zone" of gob. The residual coal and gangue are completely compressed by the overlying stratum that has lost the hinge function. The reduced porosity and air leakage result in an area that is unfavorable for spontaneous combustion. Based on the PFC^{3D} simulation of the overlying stratum collapse and porosity evolution, it can be concluded that the gob behind the working face enters the spontaneous combustion risk zone at ~160 m. The simulation results of the overlying stratum collapse and porosity provide a basis for the study on the 3D spatiotemporal distribution of the flow field in the gob.

3.3. Simulation of Flow Field Distribution behind Working Face

Before the numerical simulation of the gob flow field distribution, it is necessary to compile the porosity conditions for each part of the 3D gob model. At present, the porosity conditions of gob numerical simulation models are usually set by two methods. The first method divides the gob and sets the corresponding porosities based on the overlying stratum collapse law and the distribution law of three horizontal zones and three vertical zones. The second method sets gob porosity using UDF.

In Section 3.2, the numerical simulation of porosity suggests that the distribution of porosity in the gob is relatively random and the studied coal seam is a near-horizontal coal seam. In addition, the hyperbolic tangent function compiled by the UDF method is symmetrical, which is more reasonable in practical applications. Therefore, this study adopts the UDF method to set the gob porosity.

How to import the PFC^{3D} simulation results into FLUENT software is the key to the application of this method. Because the porosity data in PFC^{3D} are unit parameters and do not require interpolation or extrapolation transformation, a data transfer program can be compiled for one-way data communication between PFC^{3D} and FLUENT. The FLUENT software can then obtain the porosity simulation results of PFC^{3D} software. With the

FLUENT software used as the main program of the calculation, the porosity data obtained with PFC^{3D} are compiled into UDF files. It is worth noting that the calculations of the two programs are not conducted at the same time as they are connected. Instead, the numerical simulation of the PFC^{3D} particle flow is carried out first to obtain the porosity parameters. The program is then compiled to import the porosity parameters into FLUENT.

The gob numerical simulation of the 31,116 working face was aimed to determine the gas distribution law in the gob under variable mining conditions by calculations, to accurately obtain the flow field distribution in the gob, and to evaluate the 3D spontaneous combustion situation in the gob based on the dynamic distribution of oxygen in the gob. The simulation results are shown in Figure 7.

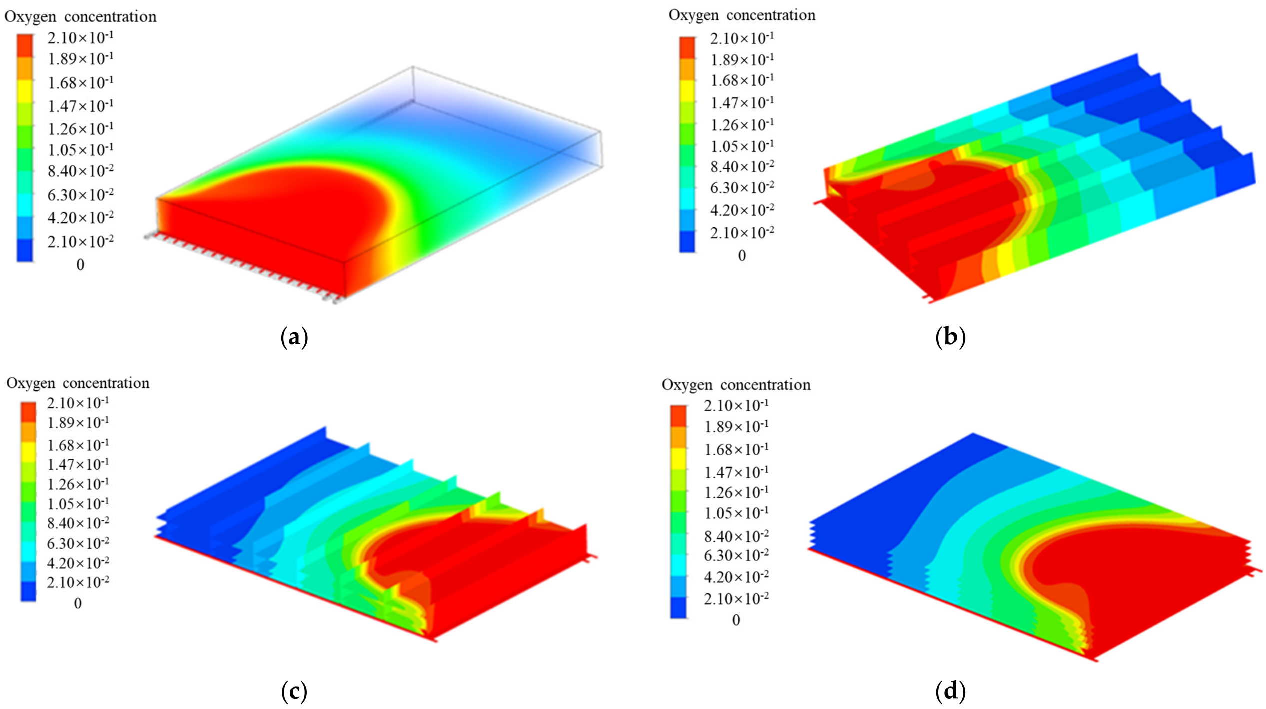

Figure 7. Oxygen concentration distribution in each axis (own elaboration). (**a**) Oxygen concentration distribution in gob. (**b**) Oxygen concentration distribution in yz-plane. (**c**) Oxygen concentration distribution in xz-plane. (**d**) Oxygen concentration distribution in z-plane.

As shown in Figure 7a, the oxygen concentration distribution in the gob is affected by the wind flow migration. Along the strike, the air seepage range in the gob shows a downward trend with the increase in gob depth. As can be seen from Figure 7b,c, in the dip direction, the seepage range of oxygen in the center of the gob is more obvious than those on the intake airway and return airway sides, and the oxidation zone reaches as deep as 351.6 m. From the view of the working face, the width of the oxidation zone shows a first decreasing and then increasing trend. The air seepage range on the return airway side is significantly higher than that on the intake airway side, contrary to the results of most studies. It can be explained that the GER process builds a flexible concrete formwork wall on the intake airway side in the gob and most of the air flow enters the entry. The air flow entering the intake airway is limited, and thus the air seepage range is significantly reduced. As shown in Figure 7d, in the vertical direction, the closer to the gob, the larger the oxygen seepage range, which can be explained with the simulation results of the overlying stratum collapse law using the PFC^{3D} particle flow software. The overlying stratum collapses as the working face advances, which increases the porosity in the upper gob. Meanwhile, rocks and gangue are accumulated and compacted in the lower gob, resulting in lower porosity in the gob bottom. Therefore, the air seepage range in the upper gob is relatively larger.

To further understand the gob flow field distribution and the cause of the hazardous area in the ultra-long working face, the distribution maps of the gob wind velocity and flow field during the mining are drawn as shown in Figure 8.

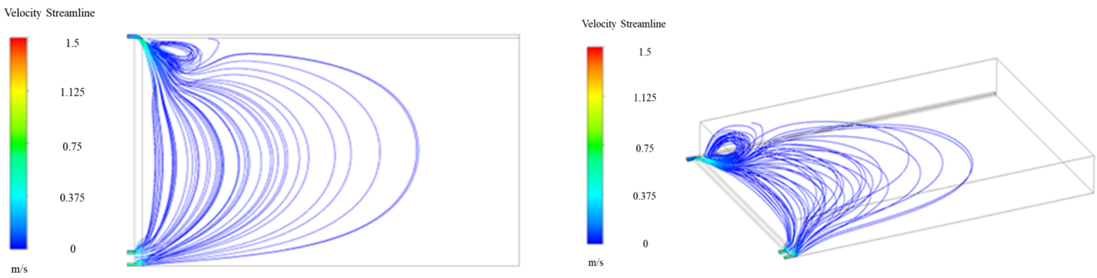

(**a**) (**b**)

Figure 8. Distribution map of wind velocity and flow field in gob during caving (own elaboration). (**a**) A 2D wind velocity field map. (**b**) A 3D wind velocity field map.

During caving, the flow field in the gob shows an arch-shaped distribution with a swirl near the intake airway that then merges with the return air flow (Figure 8). It is possibly caused by the GER process. With the advancement of the working face, flexible concrete framework walls are built immediately behind the end support to enhance the support for the roof, which makes the stratum collapse near the intake airway difficult and results in large porosities and more concentrated wind flows. As can be seen from Figure 8a, the roof rock in the gob collapses and is compacted with the advance of the working face and the air leakage flow in the gob gradually becomes weaker. In the vertical direction, the wind flow in the upper gob is stronger than those in the middle and lower gob (Figure 8b), consistent with the PFC^{3D} simulation results of porosity and oxygen distribution. After mining, the porosity of the upper gob becomes larger than those of the middle and lower parts because overlying stratum is collapsed and the collapsed rocks are gradually compacted at the lower gob.

The comparison of the oxygen concentration changes at the four measuring points and the numerically simulated flow field distribution of the gob suggests that the differences of the points of different gob parts where the residual coals enter the oxidation zone are small. Therefore, identifying the hazardous zone of spontaneous combustion of residual coal in gob by analyzing the dynamic evolution of gob porosity and changes in the gob flow field is feasible and reliable.

4. Discussion

The distribution range of the hazardous zone of residual coal spontaneous combustion is affected by many factors, and the distribution of oxygen concentration alone is insufficient for identifying the zone. Therefore, the distribution of residual coal is included in our study to determine the spontaneous combustion hazardous area. The caving rate of the studied working face is 95% and the bulk density of coal is 1.29 t/m^3. After the working face is mined, the amount of residual coal in the gob is calculated to be 270,000 m^3. The key areas of residual coal distribution provide good material conditions for the spontaneous combustion of residual coal. When air leakage passes through this area, more heat will be generated, resulting in a rapid accumulation of heat and a stronger risk of spontaneous combustion. Therefore, it is necessary to locate the key distribution areas of the residual coal. Theoretically, the residual coals are mainly distributed in the two consecutive roadways and the points of slope gradient change, since the working face does not pass any faults. The simulations have identified the spontaneous combustion oxidation zone in the gob ranging from 140.4 m to 313.3 m on the intake airway side, from 201.2 m to 351.6 m in the middle, and from 153.2 m to 328.1 m on the return airway side. Therefore, the oxygen concentration distribution and the distribution of residual coal are superimposed, with the former as the main factor, and the schematic diagram of the coal spontaneous combustion hazardous zone in the gob is drawn using the Surfer software as shown in Figure 9.

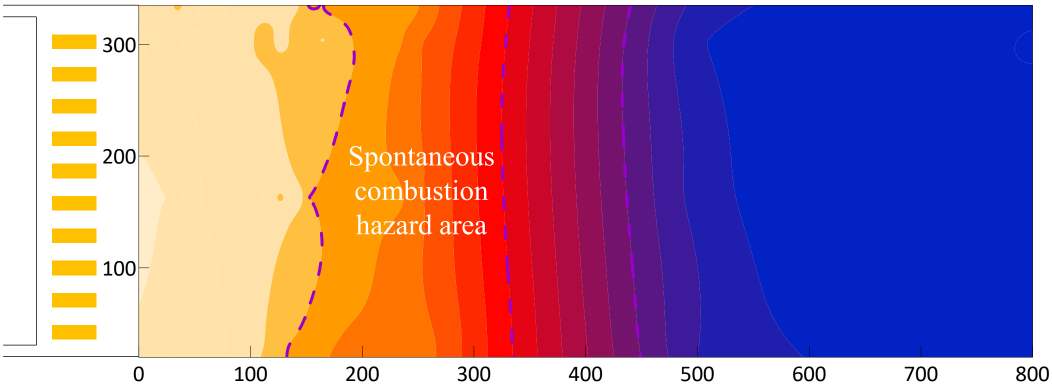

Figure 9. Distribution of coal spontaneous combustion hazardous zone in the gob (own elaboration).

Compared to previous studies, this study mainly focuses on the actual characteristics of the overlong working face on the spot and studies the flow field in the goaf and the distribution of hazardous areas, filling the gap in the current research on the distribution of hazardous areas. The research results provide theoretical guidance for the fire prevention and extinguishing work in this mine and mines with similar conditions, which is conducive to proposing targeted fire prevention and extinguishing technologies, reducing fire prevention costs, and ensuring safe production in the mine.

5. Conclusions

This study uses the method of combining on-site monitoring and numerical simulation to establish a three-dimensional numerical model of the goaf, master the collapse law of the overlying strata and the evolution law of porosity during the mining process of the ultra-long working face, elaborate the space–time evolution law of the three-dimensional flow field in the goaf of the ultra-long working face, and combine the distribution of oxygen and residual coal to accurately divide the risk area of spontaneous combustion in the goaf of the ultra-long working face.

(1) The oxygen concentrations on the intake airway and return airway sides and the middle gob were measured on site using the high-pressure rubber hoses embedded in the working face. The results show that 1# and 2# measuring points enter from the heat dissipation zone to the oxidation zone as they advance to 136.4 m and 158.1 m, respectively. The 3# measuring point does not enter the oxidation zone until advancing to 210.2 m because it is close to the return airway. The 4# measuring point evolves to the oxidation zone at the depth of 160.1 m, where the oxygen concentration drops from 19.29% to 17.85%.

(2) The collapse of overlying stratum and the evolution distribution of the porosity in the gob were explored by numerical simulation using the PFC3D particle flow software. The results suggest that the growth of fractures in each rock formation slows down after caving but the number of fractures continues to increase. After the stratum collapse is completed, the collapsed rocks continue to accumulate and, eventually, the number of fractures is reduced to a stable value. The porosity becomes stable at ~0.45, ~3.5 times that of the unmined coal seam. The gob enters the spontaneous combustion hazardous zone at 160 m behind the working face.

(3) The simulation using FLUENT software reveals the distribution law of gob flow field. The wind flow field shows an arch-shaped distribution with a swirl shape on the intake airway side. As the working face advances, the wind flow gradually becomes

weaker and the air seepage range declines in the strike direction. In the dip direction, the air seepage range on the return airway side is obviously higher than that on the intake airway side. In the vertical direction, the flow field range in the upper gob is larger than those in the middle and lower gob.

(4) Residual coals are mainly distributed in the two consecutive roadways and the points of slope gradient change. The oxidation zone is determined to be in the range of 140.4–313.3 m on the intake airway side, 201.2–351.6 m in the middle of the gob, and 153.2–328.1 m on the return airway side. The hazardous zone of residual coal spontaneous combustion is then drawn by superimposing the oxygen concentration distribution and residual coal distribution, with the former as the main factor.

Author Contributions: All authors contributed to this paper. Conceptualization, S.X. and G.W.; methodology, E.W.; validation, S.X., G.W. and E.W.; formal analysis, Q.H. and M.X.; investigation, S.X.; writing—original draft preparation, S.X.; writing—review and editing, G.W.; supervision, Q.H.; funding acquisition, G.W. All authors have read and agreed to the published version of the manuscript.

Funding: The authors would like to acknowledge the support of the project of National Natural Science Foundation of China (No. 51974176, No. 52174194, No. 51934004), Taishan Scholars Project (TS20190935), Shandong outstanding youth fund (ZR2020JQ22).

Data Availability Statement: The data used for conducting classifications are available from the corresponding author upon request.

Conflicts of Interest: The authors declare no potential conflict of interest with respect to the research, authorship, and publication of this article.

References

1. Wang, G.; Xie, S.; Huang, Q.; Wang, E.; Wang, S. Study on the performances of fluorescent tracers for the wetting area detection of coal seam water injection. *Energy* **2023**, *263*, 126091. [CrossRef]
2. Wang, H.; Chen, C. Experimental study on greenhouse gas emissions caused by spontaneous coal combustion. *Energy Fuels* **2015**, *29*, 5213–5221. [CrossRef]
3. Ding, Y.; Huang, B.; Li, K.; Du, W.; Lu, K.; Zhang, Y. Thermal interaction analysis of isolated hemicellulose and cellulose by kinetic parameters during biomass pyrolysis. *Energy* **2020**, *195*, 117010. [CrossRef]
4. Shao, X.; Qin, B.; Shi, Q.; Yang, X.; Ma, Z.; Xu, Y.; Hao, M.; Jiang, Z.; Jiang, W. Study on the sequestration capacity of fly ash on CO_2 and employing the product to prevent spontaneous combustion of coal. *Fuel* **2023**, *334*, 126378. [CrossRef]
5. Rongkun, P.; Li, C.; Chao, J.; Hu, D.; Jia, H. Thermal properties and microstructural evolution of coal spontaneous combustion. *Energy* **2023**, *262*, 125400.
6. Shi, Q.; Qin, B.; Hao, Y.; Li, H. Experimental investigation of the flow and extinguishment characteristics of gel-stabilized foam used to control coal fire. *Energy* **2022**, *247*, 123484. [CrossRef]
7. Shi, Q.; Qin, B.; Xu, Y.; Hao, M.; Shao, X.; Zhuo, H. Experimental investigation of the drainage characteristic and stability mechanism of gel-stabilized foam used to extinguish coal fire. *Fuel* **2022**, *313*, 122685. [CrossRef]
8. Wang, G.; Liu, Q.; Sun, L.; Song, X.; Du, W.; Yan, D.; Wang, Y. Study on Secondary Oxidation Spontaneous Combustion Characteristics of Coal Based on Programmed Temperature Experiment. *J. Energy Resour. Technol.* **2018**, *140*, 082204. [CrossRef]
9. Wang, G.; Yan, G.; Zhang, X.; Du, W.; Huang, Q.; Sun, L.; Zhang, X. Research and development of foamed gel for controlling the spontaneous combustion of coal in coal mine. *J. Loss Prev. Process Ind.* **2016**, *44*, S0950423016303060. [CrossRef]
10. Kim, C.J.; Sohn, C.H. A novel method to suppress spontaneous ignition of coal stockpiles in a coal storage yard. *Fuel Process. Technol.* **2012**, *100*, 73–83. [CrossRef]
11. Antoshchenko, M.; Tarasov, V.; Nedbailo, O.; Zakharova, O.; Yevhen, R.J.M.D. On the possibilities to apply indices of industrial coal-rank classification to determine hazardous characteristics of workable beds. *Min. Miner. Depos.* **2021**, *15*, 1–8. [CrossRef]
12. Antoshchenko, M.; Tarasov, V.; Rudniev, R.; Zakharova, O. Using indices of the current industrial coal classification to forecast hazardous characteristics of coal seams. *Min. Miner. Depos.* **2022**, *16*, 7–13. [CrossRef]
13. Zhang, X.; Zou, J. Research on collaborative control technology of coal spontaneous combustion and gas coupling disaster in gob based on dynamic isolation. *Fuel* **2022**, *321*, 124123. [CrossRef]
14. Xie, Z.; Cai, J.; Zhang, Y. Division of Spontaneous Combustion “Three-zone” in Gob of Fully Mechanized Coal Face with Big Dip and Hard Roof. *Procedia Eng.* **2012**, *43*, 82–87. [CrossRef]
15. Wen, H.; Wang, W.; Tao, W.; Cheng, X.; Jiang, X.; Cheng, B. Study on coal spontaneous combustion prediction and control technology during withdrawal period of super long fully-mechanized mining face. *Coal Sci. Technol.* **2020**, *48*, 167–173.

16. Wolf, K.-H.; Bruining, H. Modelling the interaction between underground coal fires and their roof rocks. *Fuel* **2007**, *86*, 27612777. [CrossRef]
17. Magdalena, T. Numerical research of oxidation zone variation in goaf of longwalls U-type system from borders and U-type system to the borders ventilated. *IOP Conf. Ser. Earth Environ. Sci.* **2019**, *221*, 1311–1323.
18. Zhuo, H.; Qin, B.; Qin, Q.; Su, Z. Modeling and simulation of coal spontaneous combustion in a gob of shallow buried coal seams. *Process Saf. Environ. Prot.* **2019**, *131*, 246–254. [CrossRef]
19. Fan, H.; Xu, H.; Wang, G.; Wang, J.; Liu, Z.; Cheng, Q. Determination of roof horizontal long drilling hole layout layer by dynamic porosity evolution law of coal and rock. *Powder Technol.* **2021**, *394*, 970–985. [CrossRef]
20. Gao, J.; Hai, P. Influence of Permeability Distribution on Airflow Field of Leakage in Gob. *China Saf. Sci. J.* **2010**, *20*, 81–85.
21. Gao, H.; Gong, X.; Cheng, X.; Yu, R.; Wang, H. Study on the reasonable arrangement of high position drilling holes based on the law of overlying rock fracture development. *Coal Eng.* **2021**, *53*, 90–93.
22. Di, S.; Zhang, S.; Cao, Y.; Xue, L. Study on Failure Form and Stress Evolution Law of Overlying Strata in Fully Mechanized Mining Face. *Shanxi Coal Coking Technol.* **2020**, *44*, 41–45.
23. Wang, G.; Wu, M.; Wang, R. Hight of the mining-induced fractured zone above a coal face. *Eng. Geol.* **2017**, *2016*, 140–152. [CrossRef]
24. Gamiy, Y.; Kostenko, V.; Zavialova, O.; Kostenko, T.; Zhurbynskyi, D. Identifying sources of coal spontaneous heating in mine workings using aerogas control automatic systems. *Min. Miner. Depos.* **2020**, *14*, 120–127. [CrossRef]
25. Zhang, Y.; Niu, K.; Du, W.; Zhang, J.; Wang, H.; Zhang, J. A method to identify coal spontaneous combustion-prone regions based on gob flow field under dynamic porosity. *Fuel* **2021**, *288*, 119690. [CrossRef]